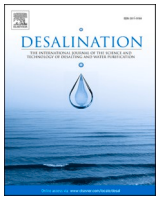
Desalination 613 (2025) 118939



Contents lists available at ScienceDirect

Desalination

journal homepage: www.elsevier.com/locate/desal



Membrane arrangement influences time to steady state in FCDI with multi-ionic salt solutions

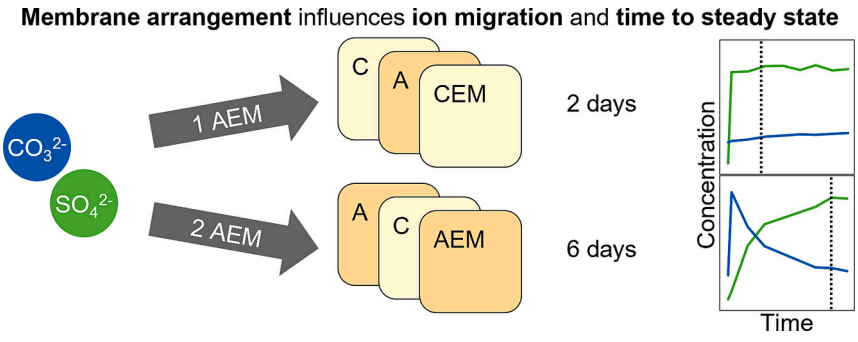
Lukas Mankertz [a,b], Meike Theis [a,b], Christian J. Linnartz [a,b], Matthias Wessling [a,b,*]

[a] Chemical Process Engineering AVT.CVT, RWTH Aachen University, Forckenbeckstraße 51, 52074 Aachen, Germany
[b] DWI - Leibniz Institute for Interactive Materials e.V., Forckenbeckstraße 50, 52074 Aachen, Germany

HIGHLIGHTS

- Modules with IEM arrangements of two CEMs and one AEM (C | A | C) or vice versa (A | C | A).
- Similar levels of desalination and concentration are reached regardless of IEM arrangement.
- Time to steady state varies drastically depending on IEM arrangement.
- Identified flow-electrode buffer and ion pathway as important process parameters in FCDI with multi-ionic salt solutions.

GRAPHICAL ABSTRACT



ARTICLE INFO

Keywords:
Flow-electrode capacitive deionization
Ion-exchange membrane
Multi-ionic salt solutions
Ion species
Selectivity
Concentration
Desalination

ABSTRACT

Flow-electrode capacitive deionization (FCDI) is a promising technology for energy-efficient desalination, offering the potential to selectively remove ions from multi-ionic salt solutions. This study presents a comparative investigation of two FCDI modules with distinct ion-exchange membrane (IEM) arrangements, using cation-exchange membranes (CEM) and anion-exchange membranes (AEM): CEM-AEM-CEM (C | A | C) and AEM-CEM-AEM (A | C | A). Both modules achieved similar levels of desalination and concentration in steady state, but the time required to reach steady state varied significantly due to differences in the IEM arrangement and the ionic buffer-capacity of the flow electrode.

The results revealed that membrane selectivity is critical in systems with multiple ion species, particularly before achieving a steady state, where conductivity alone proves insufficient for characterizing salt composition. A higher selectivity for sulfate over carbonate was observed for AEMs, causing delayed stabilization of concentrations in the A | C | A module. Strategies to reduce the ionic buffer-capacity of the flow electrode, such as decreasing its volume as well as recognizing which ion should follow the flow-electrode path were identified as potential means to accelerate steady-state achievement.

Furthermore, experiments with varying carbonate-to-sulfate molar ratios in the diluate feed confirmed the inherent selectivity of AEMs for sulfate and established an upper limit for normalized transport ratios. These findings emphasize the need for complementary approaches, such as membrane coatings or tailored flow-electrode materials, to enhance process selectivity and efficiency. This work provides critical insights into the

* Corresponding author at: Chemical Process Engineering AVT.CVT, RWTH Aachen University, Forckenbeckstraße 51, 52074 Aachen, Germany
E-mail address: manuscripts.cvt@avt.rwth-aachen.de (M. Wessling).

https://doi.org/10.1016/j.desal.2025.118939
Received 6 February 2025; Received in revised form 27 March 2025; Accepted 19 April 2025
Available online 1 May 2025
0011-9164/© 2025 The Authors. Published by Elsevier B.V. This is an open access article under the CC BY-NC license (http://creativecommons.org/licenses/by-nc/4.0/).

interplay of IEM arrangement and flow-electrode behavior, offering a foundation for optimizing FCDI systems in desalination applications involving complex salt solutions.

1. Introduction

Energy-efficient and scalable saltwater desalination technologies are in stark demand due to the global freshwater crisis [1]. Electromembrane technologies such as electrodialysis (ED) and (membrane) capacitive deionization ((M)CDI) are more energy-efficient than common technologies such as evaporation and crystallization while being less susceptible to membrane scaling compared to pressure-driven processes like reverse osmosis (RO) and nanofiltration (NF) [2–6]. Ion adsorption behavior in CDI is adaptable, as it can be tuned by surface properties of the porous electrode [7–12]. Compared to ED, no reactions take place at the electrodes in MCDI when the ions are moved by an electric field to the electrode surfaces, where they form electrical double layers, allowing for even higher energy efficiency [2,4,9,13,14].

While MCDI cannot operate continuously, flow-electrode capacitive deionization (FCDI) has received attention in the research community due to its potential for continuous desalination [4,9,15]. FCDI relies on the electrostatic adsorption of ions onto flowable activated carbon electrodes while applying an electrical potential, offering an energy-efficient mechanism for saltwater desalination. FCDI utilizes ion-exchange membranes (IEM) to selectively remove ions from a feed stream. [16,17] In 2015, a single module layout was introduced to the FCDI research community, allowing for continuous concentration and desalination [18]. In 2023, the technology was scaled up to pilot-plant level for industry-relevant testing [19]. Recently, design of cell architecture, flow electrode and current collectors were identified as potential for increasing process efficiency in FCDI [20–22]. For salt recovery applications, the ion selectivity of the FCDI process is of great importance, as it opens the door for concentrating desired salts while leaving undesired salts in the diluate for a subsequent separation.

One way to influence the selectivity of the process is by the IEMs used in FCDI. IEMs are critical components in electromembrane processes for hydrogen production and water treatment [4,23–26]. IEMs contain charged groups, allowing the selective passage of so-called counter-ions of opposite charge, while co-ions of the same charge as the IEMs are retained [27]. The selective permeation of ions in ED was shown to be mainly dependent on the degree of affinity of the ion to the specific IEM [28]. So far, several steps have been undertaken to investigate the influences of IEMs in capacitive deionization processes. IEMs have received attention in modeling and simulation of steady-state FCDI processes using single salt solutions with low- and high salinity, showing that the performance of IEMs with different characteristics regarding diffusion coefficients, osmotic permeability, and stern capacity can be predicted to aid the development of such membranes [29,30]. A cross-linked coating for a cation-exchange membrane (CEM) was subsequently introduced to mitigate water crossover [31]. The functional design of IEMs has been identified as a critical aspect for further research [32].

FCDI has been utilized for selective separation of phosphorus and copper ions in a wide range of concentrations [12,33]. The investigation of selective removal of sodium and calcium ions via layer-by-layer coating of CEM yielded different affinities toward mono- or divalent ions [34]. The influence of CEM and anion-exchange membrane (AEM) arrangements on desalination performance with NaCl and potassium chloride solutions has been investigated numerically and experimentally, showing that a CEM-AEM-CEM arrangement yields higher desalination rates [35].

The publications mentioned above show that the effectiveness of desalination in FCDI processes is influenced not only by the salinity of the feed but also by the choice and modification of IEMs, as well as by the configuration of the system in terms of membrane arrangement. A different membrane arrangement significantly impacts the process environment. However, the exact behavior of multi-ionic salt solutions in feed and flow-electrode streams in a single module FCDI setup [18] with different membrane arrangements is yet to be investigated.

This work aims to highlight the impact of different membrane arrangements and the ionic buffer-capacity of the flow electrode on the FCDI process. Two configurations are investigated: a CEM-AEM-CEM (C | A | C) arrangement and an AEM-CEM-AEM (A | C | A) arrangement in a single-module FCDI setup (see Fig. 1). IEMs exhibit varying selectivities toward different ions, complicating the treatment of multi-ionic salt solutions.

Understanding the process behavior and ion selectivity in different membrane arrangements is essential for optimizing FCDI systems to address the challenges posed by diverse water sources and compositions. In this context, multi-ionic salt solutions containing different anions (carbonate and sulfate) are investigated. These salt solutions represent wastewater streams generated during polycarbonate production processes, providing a relevant case study for industrial applications.

2. Experimental

We use FCDI modules based on the above single module layout, with varying IEM arrangements. The membranes are CEMs (Fumasep FKS-PET-130, Fumatech BWT GmbH) and AEMs (Fumasep FAS-PET-130, Fumatech BWT GmbH), with an individual surface area of 100 cm^2. Depending on the configuration of the module, two CEMs and one AEM are used (C | A | C) or vice versa (A | C | A), see Fig. 2.

These modules are comprised of 180x180x10mm graphite plates (Müller & Rössner GmbH & Co. KG) with milled meandering flow channels. The unprocessed surface of the graphite plates is coated with an insulator (Plastik 70; Kontakt Chemie GmbH) to prevent electrically induced damage to the adjacent IEMs. The solutions are distributed in the module through mesh spacers (ED-100 spacer; Fumatech BWT GmbH), which comprise the concentrate and the diluate channel. The feed streams are transported through the module using a two-channel peristaltic pump (Cole-Parmer™ Ismatec™ Reglo ICC; Fisher Scientific International Inc.). Each channel is operated at a different flow rate. The flow rate is set to 1.5 mL/min for the diluate and 0.05 mL/min for the concentrate. The salt solutions for the feed streams consist of 22 g/L Na_2CO_3 and 100 g/L Na_2SO_4 in the diluate and 22 g/L Na_2CO_3 in the concentrate, solved in ultrapure water, respectively. The flow electrode consists of 76.5 g/L Na_2CO_3 in ultrapure water and 15 $wt\%$ of activated carbon powder (Carbopal SC11PG; Donau Carbon GmbH), with a total flow-electrode volume of 600 mL. Using Na_2CO_3 in the flow electrode was chosen as it was the desired salt for recovery in this case. Flow-electrode solutions are stirred for a minimum of 24 h prior to the beginning of and during an experiment to prevent sedimentation and agglomeration. A peristaltic pump (Masterflex™ Easy-Load II; Fisher Scientific International Inc.) is used to circulate the flow electrode in a closed loop at a set flow rate of 250 mL/min. A current of 0.35A is applied to the graphite plates using a DC power supply (E3644A; Keysight Technologies) through banana plug cables. Experiments are conducted over 7 days to investigate the influence of IEM arrangement on desalination and concentration performance over an extended period of time. Conductivity sensors (Knick SE 615/1MS; Knick Elektronische Messgeräte GmbH & Co. KG) are used to measure the conductivity and temperature of the diluate and concentrate outlet streams. Conductivity serves as a metric to recognize the desalination and concentration state during FCDI. Quantitative sample analysis is performed using ion chromatography (930 Compact IC Flex, anion column: Metrosep A Supp 7–250/4.0, cation column: Metrosep C 6–250/4.0; Metrohm

Deutschland GmbH & Co. KG) for sodium and sulfate ions and total organic carbon analysis using a non-dispersive infrared sensor (TOC-LCPH High Sensitivity Model; Shimadzu Scientific Instruments) for carbonate. Flow-electrode samples are filtered by filter paper (Qualitative filter paper 413; VWR International) with a particle retention of 5 – 13 μm before analysis. For process- as well as desalination and concentration performance, respectively, monitored conductivities and measured concentration values serve as a basis for comparison. A transfer ratio and normalized transfer ratio are calculated to determine the influence of the anion feed ratio. Relevant equations are detailed in the supplementary information S1.

3. Results and discussion

Below we investigate and report the overall desalination performance of two FCDI modules. The first module consists of two CEMs and one AEM, referred to as the C | A | C configuration. The second module utilizes two AEMs and one CEM, referred to as the A | C | A configuration.

A long-term experiment is conducted for each configuration using identical starting parameters as described earlier. Fig. 3 presents the conductivity profiles recorded during these experiments, with separate data illustrating the conductivity trends for the concentrate and diluate channels.

Both conductivity graphs indicate no significant change in the diluate conductivity. This behavior is attributed to the faster flow rate of the diluate compared to the concentrate. In contrast, the concentrate conductivity exhibits an initial sharp increase, followed by a period of stable conductivity. Differences in the magnitude of conductivity suggest a higher total salt concentration in the concentrate of the A | C | A module. These differences may be due to deviations in the initial feed solution concentrations or could indicate slightly improved performance of the A | C | A module. Potentials are monitored throughout the experiment duration for both modules and are shown in the supplementary information S2.

Typically, stable conductivity signals that the desalination process has reached a steady state, where ion adsorption and desorption at the flow-electrode surfaces are in equilibrium. This steady state implies that the desalination and concentration processes are stable under the current process parameters. However, ion concentrations must be analyzed alongside conductivity to conclusively confirm the steady state of the desalination process.

Fig. 4 presents the concentration profiles of the anions in the diluate and concentrate throughout the experiments for both the C | A | C and A | C | A modules.

In the concentrate of the C | A | C module, carbonate concentration shows a linear increase throughout the experiment. Sulfate anions are not present in the concentrate feed at the start of the experiment. A sharp increase in sulfate concentration in the concentrate is observed after 5 h and does not change significantly after 2 days. The diluate sulfate concentration experiences a slight decrease during the same time. Both

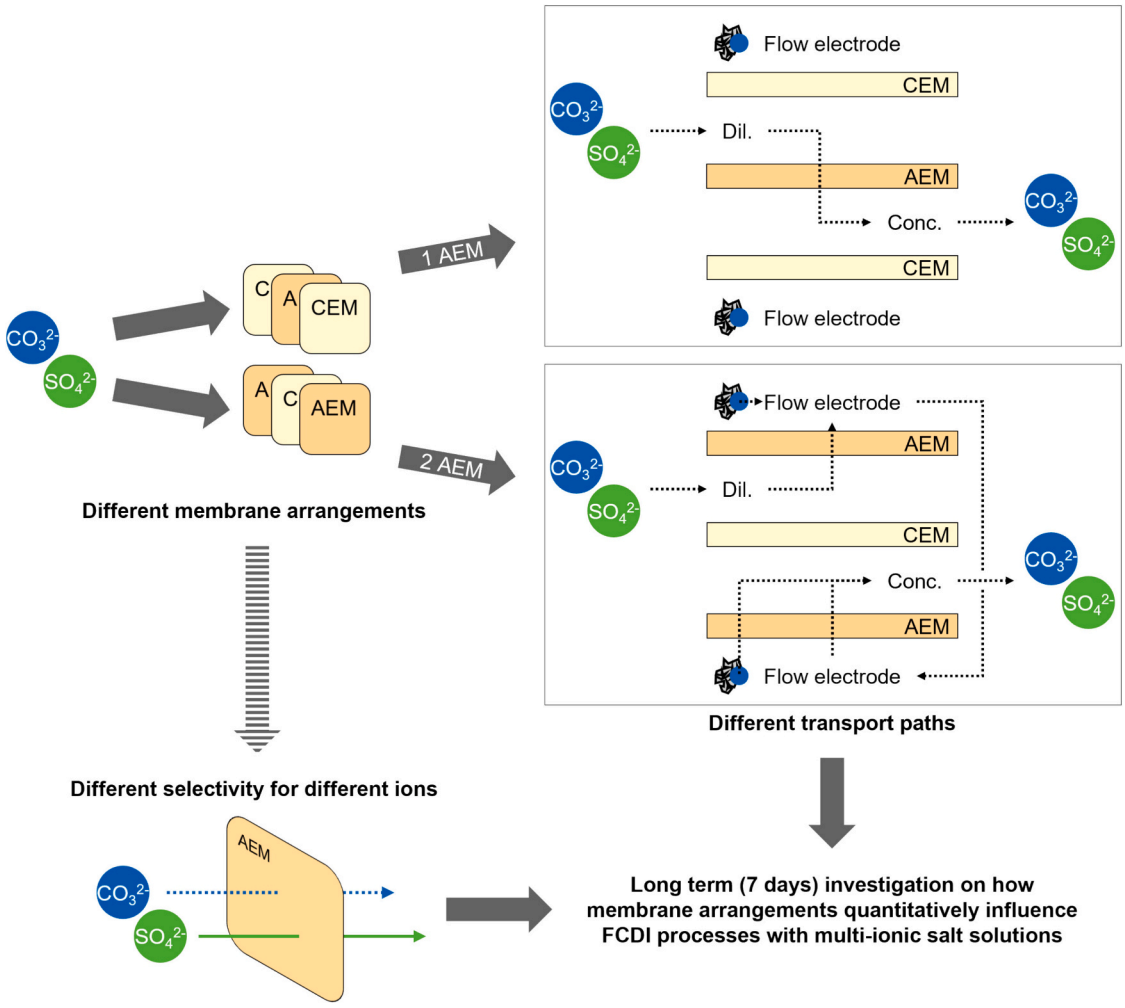


Fig. 1. The influence of different membrane arrangements in FCDI with multi-ionic salt solutions is yet to be investigated. The figure depicts possible membrane arrangements and resulting anion-transport routes in a two-compartment FCDI cell. With long-term experiments, these membrane arrangement conditions are to be quantitatively investigated. Dil. = diluate, Conc. = concentrate.

concentrate and diluate sulfate concentrations remain near constant afterward. Carbonate concentration in the diluate shows little change over the entire duration. The collected data corresponds well with the conductivity graph shown before. The A | C | A diluate concentrations mirror those of the C | A | C module, albeit with slightly higher concentrations. On the other hand, concentrations in the concentrate exhibit a significant change. While the first concentrate sample observes a maximum carbonate concentration after 5 h, the concentration drops to near-feed values after 7 days. The sulfate concentration reaches its maximum after 6 days. Since the graphs show no significant changes after 6 to 7 days, a concentration-wise steady state is assumed to be in effect after that period. While Fig. 3 (b) shows a steady state of outlet conductivities after 2 days, Fig. 4 (b) demonstrates that it takes 6 days to reach stable concentrations in the A | C | A module. From similar and stable levels of diluate and concentrate conductivities and concentrations after reaching steady state in different amounts of time, it can be assumed that no membrane degradation or fouling occurred in the 7 days of experiments. However, the lifetime of IEMs in FCDI operation on a grander time scale is yet to be investigated. The anion concentrations in the flow electrodes must be investigated to understand the development in the A | C | A module. These are given in Fig. 5 for both modules. Anion transport occurs solely across one membrane in the C | A | C module. In the A | C | A module, anions have to migrate across two AEMs before reaching the concentrate, as shown in Fig. 2. The first AEM separates the diluate and the flow electrode, with the diluate on the feed side and the flow electrode on the permeate side. The flow electrode subsequently functions as the feed stream for the second AEM, which separates flow electrode and concentrate.

For the flow electrode used in the C | A | C arrangement, there is no observed change in carbonate or sulfate concentrations between the first and final samples, indicating that sodium cations facilitate charge transport through the flow electrode as intended. Furthermore, the CEMs exhibit high retention of co-ions, allowing little to no migration of carbonate or sulfate anions out of or into the flow electrode, respectively.

In the A | C | A arrangement, the carbonate concentration in the flow electrode decreases throughout the experiment, while the sulfate concentration increases. Initially, as the flow electrode contains no sulfate ions, all charge transport from the flow electrode to the concentrate is facilitated by carbonate ions. This results in a rapid increase in carbonate concentration in the concentrate shortly after the experiment begins, as previously described. As sulfate ions migrate into the flow electrode, this effect gradually transfers to the concentrate, driven by the selectivity of the AEMs. This behavior underscores a significant difference in AEM selectivity between carbonate and sulfate, with sulfate exhibiting preferential transport. Consequently, the initially high carbonate concentration in the A | C | A concentrate is eventually replaced by sulfate as sulfate concentrations in the flow electrode increase.

To achieve a steady state, an equilibrium of ion adsorption and desorption within the flow electrode is necessary. In the A | C | A module, the selectivity of the second AEM (separating the flow electrode and concentrate) aligns with the selectivity of the first AEM (separating the diluate and flow electrode) over time. The inherent ionic buffer-capacity of the flow electrode delays this alignment. A potential approach to reduce buffer capacity and shorten process time is to decrease the flow-electrode volume, leading to a lower absolute amount of carbonate ions available for transport. Additionally, starting with a higher initial sulfate concentration in the flow electrode could mitigate the time-gating effect. Independent of the salt ions used in this study, the fastest ion should follow the path over the flow electrode in FCDI because its higher ionic mobility and diffusion coefficient allow it to respond more quickly to the applied electric field and the ad- and desorption to and from the flow electrode, minimizing resistance and enhancing charge transfer efficiency. However, if there is only one cation and multiple anions or vice versa, the single ion species should be the one to take the flow-electrode path to avoid the influence of flow-electrode buffer. A detailed investigation of the buffer capacity of flow electrodes in multi-ionic salt solutions should be subject to future research.

It can be argued that in FCDI with multi-ionic salt solutions, faster ions are preferred for concentration purely from a process design point of view. Future work should explore this hypothesis as well as whether specifically tailored multi-ionic salt solutions can accelerate the stabilization of concentrations. These findings also prompt an investigation of the influence of carbonate and sulfate feed concentrations on the selectivity of a single AEM. To address this, experiments were conducted with increasing carbonate-to-sulfate molar ratios in the diluate feed. Since only a single AEM is being examined, the experiments were carried out using the C | A | C module, which allows for shorter durations as a steady state is reached more quickly. To eliminate potential errors from premature sampling, all experiments were conducted for 56 h. Fig. 6 presents the anion concentrations and transfer ratios obtained across varying carbonate-to-sulfate molar ratios in the diluate feed.

Since the concentrate feed concentration, flow rates, and applied current are kept constant across all experiments, it can be concluded that the molar ratios of carbonate to sulfate in the diluate feed play a significant role in determining the achievable concentrations and, consequently, the selectivity of the membrane. However, increasing the diluate feed anion ratio of carbonate to sulfate by a factor of 20 results in only a fourfold increase in carbonate concentrations. This becomes evident when comparing the ionic fluxes of the two anions.

The transfer ratio indicates a higher ionic flux of carbonate compared to sulfate across the AEM at higher diluate feed anion ratios. However, the feed concentration directly affects ion availability for transport and must be accounted for in the analysis. When normalized to the diluate

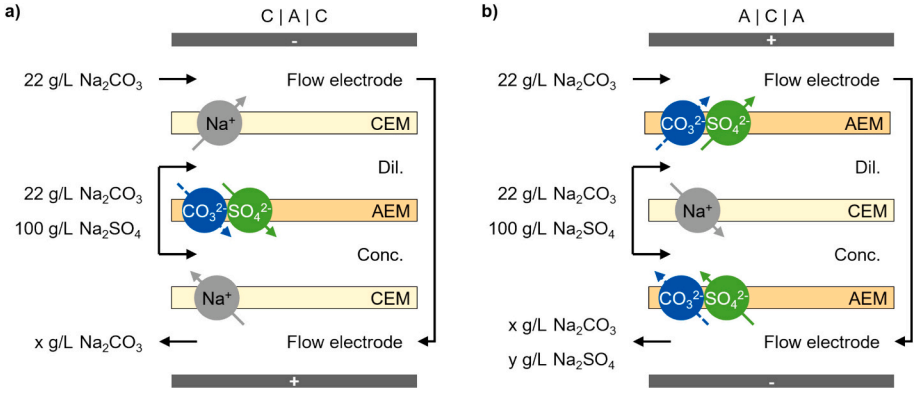


Fig. 2. FCDI module configuration with ions (non-stoichiometric cation to anion ratio, current collectors, membranes and solution streams: (a) C | A | C module with two CEMs and one AEM leading to cation transport via the flow electrode, (b) A | C | A module with two AEMs and one CEM leading to anion transport via the flow electrode.

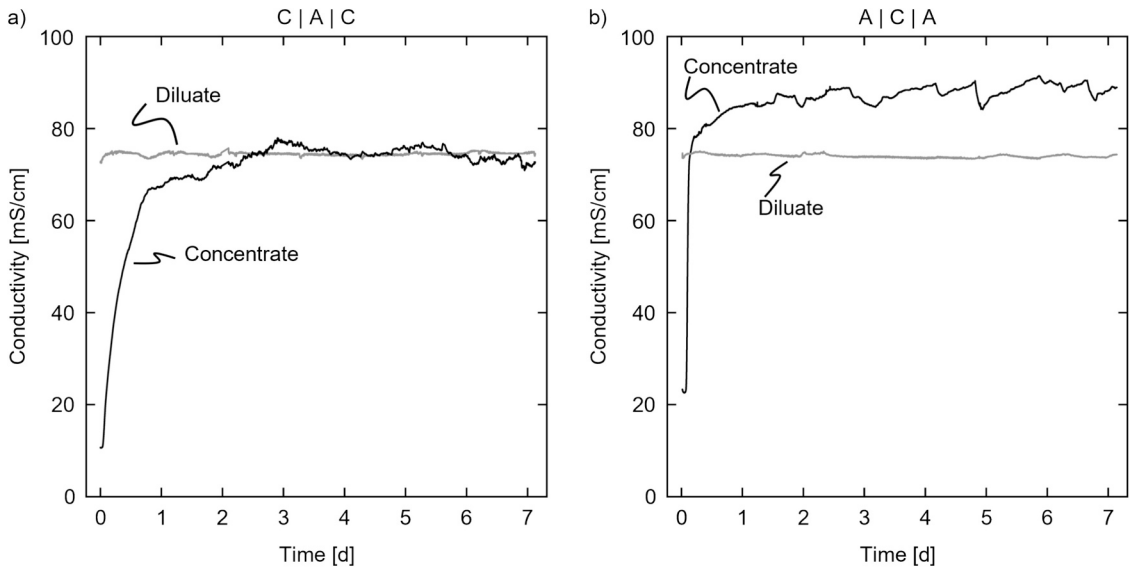


Fig. 3. Conductivity of both concentrate (black) and diluate channel (grey) for the C | A | C module (a) and A | C | A module (b) over the experiment duration of 7 days.

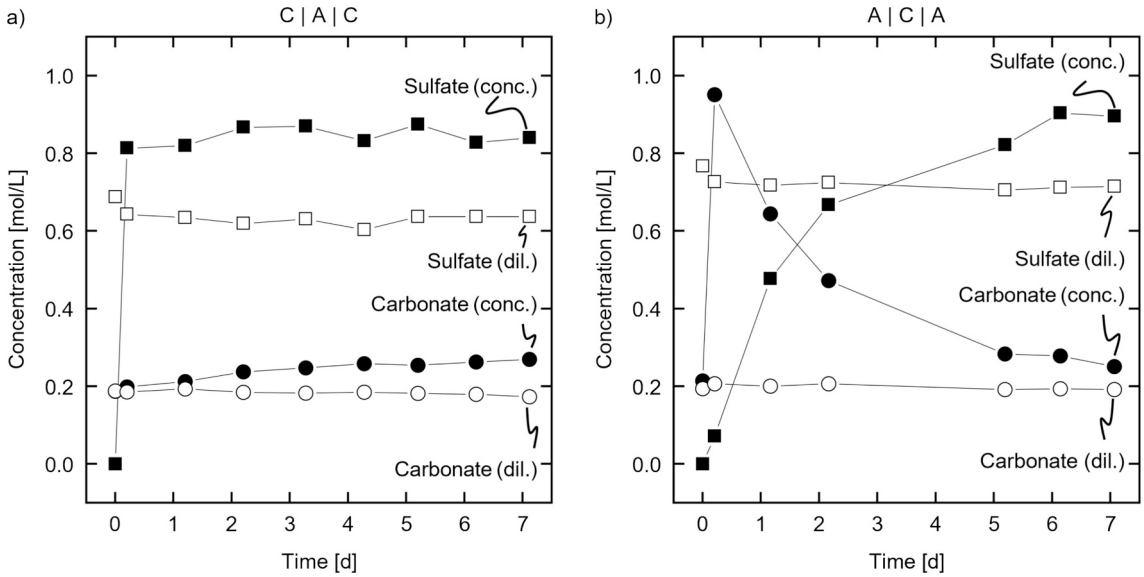


Fig. 4. Anion concentrations in the concentrate (conc.) and diluate (dil.) channels of the C | A | C module (a) and A | C | A module (b) over the experiment duration of 7 days.

feed concentration, the transport ratio values appear to approach an upper limit of approximately 0.5 *mol* of carbonate per 1 *mol* of sulfate transported. This observation confirms that the AEM exhibits higher selectivity toward sulfate.

Future research should explore the applicability of these results to the A | C | A arrangement. With the salt composition used in this study, the flow-electrode may have a more pronounced influence on the system's overall performance and ion transport behavior.

4. Conclusion

The comparative investigation of two FCDI modules with different IEM arrangements during long-term continuous operation revealed that both the C | A | C and A | C | A modules achieve comparable concentration and desalination levels at steady state. However, the time required to reach steady state varies significantly between the two configurations, primarily due to differences in IEM arrangement and the buffering effect of the flow electrode. When multiple anions migrate through the flow electrode, selectivity becomes critical in determining the steady-state behavior. While the impact of different cations remains unexplored, it is hypothesized that their behavior may be analogous.

Relying solely on conductivity measurements is insufficient for characterizing the steady state of systems with multiple ion species. Stable conductivity provides insight into overall salt concentration but does not capture changes in salt composition. As demonstrated in this study, this limitation can obscure significant shifts in the composition of multi-ionic salt solutions over extended periods. This highlights the need for a more nuanced approach to evaluating steady state in such systems and underscores the importance of tailoring FCDI membrane arrangements and flow-electrode compositions to specific applications.

Although steady state itself is unaffected by IEM arrangement once achieved, the time required to reach a new steady state following process changes is prolonged and depends heavily on the salt concentration within the flow electrode. Reducing the total volume of the flow

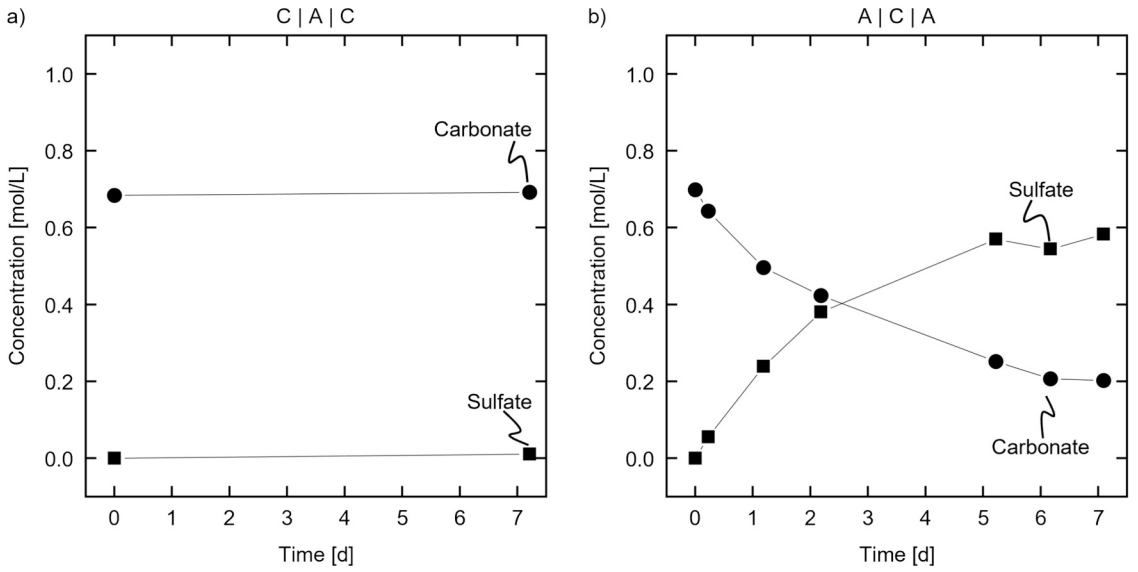


Fig. 5. Anion concentrations in the flow electrode of the C | A | C module (a) and A | C | A module (b) over the experiment duration of 7 days.

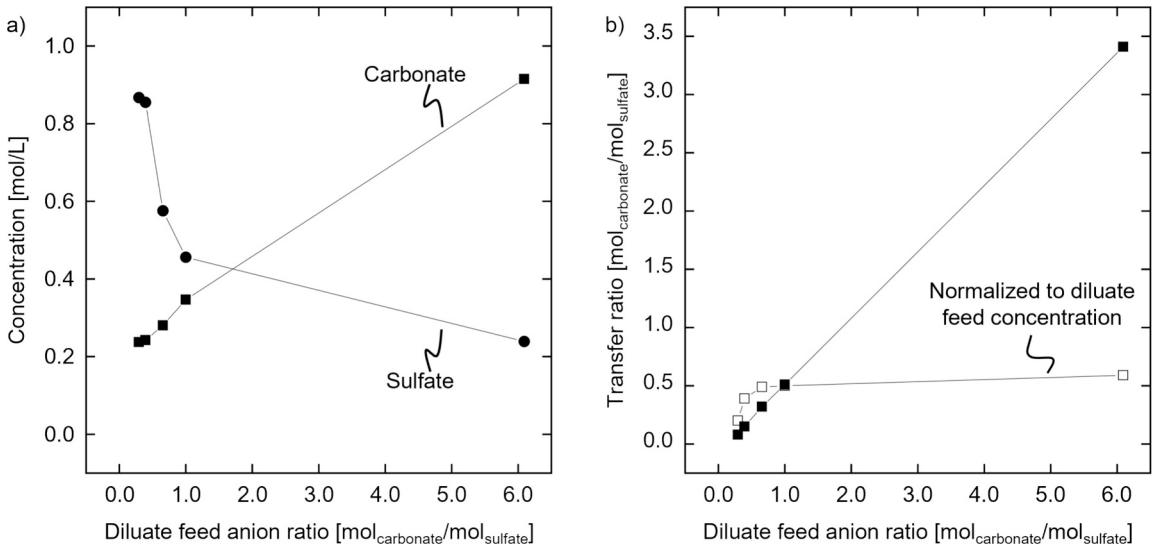


Fig. 6. Anion concentrations in the concentrate (a) and anion transfer ratio (b) in the C | A | C module at different feed concentration ratios in the diluate channel. The transfer ratio is shown both as is and normalized to the diluate feed concentration. Data connected by lines to guide the reader's eye.

electrode and optimizing flow rates could decrease this reaction time, providing a potential approach for future work and improved process design. However, IEM arrangement is not a direct tool for influencing selectivity in FCDI; selectivity is an inherent property of the IEM itself.

For systems involving multiple cations and anions, the configuration of the FCDI module alone may be insufficient to achieve desired desalination outcomes, particularly when constrained by IEM selectivity. Alternative strategies, such as applying membrane coatings or modifying flow-electrode properties through material enhancements or alternative designs, must be considered to optimize selectivity. The fastest ion should follow the flow-electrode path due to its high mobility and diffusion, optimizing charge transfer and minimizing resistance. These approaches are essential for addressing the interactions between diverse ion species and ensuring the effectiveness of electro-membrane desalination processes, particularly for complex salt solutions.

CRediT authorship contribution statement

Lukas Mankertz: Conceptualization, Data curation, Formal analysis, Investigation, Methodology, Project administration, Supervision, Validation, Visualization, Writing – original draft, Writing – review & editing. **Meike Theis:** Data curation, Investigation, Visualization. **Christian J. Linnartz:** Conceptualization, Data curation, Formal analysis, Funding acquisition, Methodology, Project administration, Supervision, Validation, Visualization, Writing – original draft, Writing – review & editing. **Matthias Wessling:** Conceptualization, Funding acquisition, Methodology, Project administration, Resources, Supervision, Writing – original draft, Writing – review & editing.

Declaration of competing interest

Matthias Wessling has patent Single module, flow-electrode apparatus and method for continous water desalination and ion separation by capacitive deionization issued to DWI - Leibniz-Institut für Interaktive Materialien e.V. Matthias Wessling has patent Electrochemical module comprising a flexible membrane-electrode assembly issued to DWI - Leibniz-Institut für Interaktive Materialien e.V. Christian Linnartz has patent Electrochemical module comprising a flexible membrane-electrode assembly issued to DWI - Leibniz-Institut für Interaktive Materialien e.V. If there are other authors, they declare that they have no known competing financial interests or personal relationships that could have appeared to influence the work reported in this paper.

Acknowledgement

This work has been supported by the German Federal Ministry of Education and Research (BMBF) under the project "RIKovery" (FKZ: 02WV1569F). M.W. acknowledges DFG funding through the Gottfried Wilhelm Leibniz Award 2019, Germany (WE 4678/12-1). The authors thank Justin Gottfried and Timo Linzenmeier for IC measurements, Stefan Herrmann and Lennart Wilms for TOC measurements as well as Niklas Bougé for the fabrication of flowfields. The authors thank Niklas Köller for critical discussion on FCDI matters.

Appendix A. Supplementary data

Supplementary data to this article can be found online at https://doi.org/10.1016/j.desal.2025.118939.

Data availability

Data will be made available on request.

References

[1] Water for Prosperity and Peace, The United Nations World Water Development Report 2024, UNESCO Publishing, Paris, ISBN 978-92-3-100657-9.
[2] Y. Oren, Capacitive deionization (CDI) for desalination and water treatment — past, present and future (a review) 228 (1) 10–29. doi:https://doi.org/10.1016/j.desal.2007.08.005. URL https://linkinghub.elsevier.com/retrieve/pii/S0011916408002294.
[3] S. Shirazi, C.-J. Lin, D. Chen, Inorganic fouling of pressure-driven membrane processes — a critical review 250 (1) 236–248. doi:https://doi.org/10.1016/j.desal.2009.02.056. URL https://linkinghub.elsevier.com/retrieve/pii/S0011916409007541.
[4] S. Porada, R. Zhao, A. Van Der Wal, V. Presser, P. Biesheuvel, Review on the science and technology of water desalination by capacitive deionization 58 (8) 1388–1442. doi:https://doi.org/10.1016/j.pmatsci.2013.03.005. URL https://linkinghub.elsevier.com/retrieve/pii/S0079642513000340.
[5] F. Macedonio, E. Drioli, Membrane engineering for green process engineering 3 (3) 290–298. doi:https://doi.org/10.1016/J.ENG.2017.03.026. URL https://linkinghub.elsevier.com/retrieve/pii/S2095809917304216.
[6] S. Zavahir, T. Elmakki, M. Gulied, Z. Ahmad, L. Al-Sulaiti, H. K. Shon, Y. Chen, H. Park, B. Batchelor, D. S. Han, A review on lithium recovery using electrochemical capturing systems 500 114883. doi:https://doi.org/10.1016/j.desal.2020.114883. URL https://linkinghub.elsevier.com/retrieve/pii/S0011916420315617.
[7] P. Długołecki, A. Van Der Wal, Energy recovery in membrane capacitive deionization 47 (9) 4904–4910. doi:https://doi.org/10.1021/es3053202. URL https://pubs.acs.org/doi/10.1021/es3053202.
[8] J.-H. Yeo, J.-H. Choi, Enhancement of nitrate removal from a solution of mixed nitrate, chloride and sulfate ions using a nitrate-selective carbon electrode 320 10–16. doi:https://doi.org/10.1016/j.desal.2013.04.013. URL https://linkinghub.elsevier.com/retrieve/pii/S001191641300180X.
[9] M. E. Suss, S. Porada, X. Sun, P. M. Biesheuvel, J. Yoon, V. Presser, Water desalination via capacitive deionization: what is it and what can we expect from it? 8 (8) 2296–2319. doi:https://doi.org/10.1039/C5EE00519A. URL https://xlink.rsc.org/?DOI=C5EE00519A.
[10] M. E. Suss, Size-based ion selectivity of micropore electric double layers in capacitive deionization electrodes 164 (9) E270–E275. doi:https://doi.org/10.1149/2.1201709jes. URL https://iopscience.iop.org/article/10.1149/2.1201709jes.
[11] E. N. Guyes, T. Malka, M. E. Suss, Enhancing the ion-size-based selectivity of capacitive deionization electrodes 53 (14) 8447–8454. doi:https://doi.org/10.1021/acs.est.8b06954. URL https://pubs.acs.org/doi/10.1021/acs.est.8b06954.
[12] X. Zhang, F. Yang, J. Ma, P. Liang, Effective removal and selective capture of copper from salty solution in flow electrode capacitive deionization 6 (2) 341–350. doi:https://doi.org/10.1039/C9EW00467J. URL https://xlink.rsc.org/?DOI=C9EW00467J.
[13] M. A. Anderson, A. L. Cudero, J. Palma, Capacitive deionization as an electrochemical means of saving energy and delivering clean water. comparison to present desalination practices: Will it compete? 55 (12) 3845–3856. doi:https://doi.org/10.1016/j.electacta.2010.02.012. URL https://linkinghub.elsevier.com/retrieve/pii/S0013468610002410.
[14] M. A. Ahmed, S. Tewari, Capacitive deionization: Processes, materials and state of the technology 813 178–192. doi:https://doi.org/10.1016/j.jelechem.2018.02.024. URL https://linkinghub.elsevier.com/retrieve/pii/S1572665718301085.
[15] F. Yang, Y. He, L. Rosentsvit, M. E. Suss, X. Zhang, T. Gao, P. Liang, Flow-electrode capacitive deionization: A review and new perspectives 200 117222. doi:https://doi.org/10.1016/j.watres.2021.117222. URL https://linkinghub.elsevier.com/retrieve/pii/S0043135421004206.
[16] S.-i. Jeon, H.-r. Park, J.-g. Yeo, S. Yang, C. H. Cho, M. H. Han, D. K. Kim, Desalination via a new membrane capacitive deionization process utilizing flow-electrodes 6 (5) 1471. doi:https://doi.org/10.1039/c3ee24443a. URL https://xlink.rsc.org/?DOI=c3ee24443a.
[17] A. Rommerskirchen, C. J. Linnartz, D. Müller, L. K. Willenberg, M. Wessling, Energy recovery and process design in continuous flow–electrode capacitive deionization processes 6 (10) 13007–13015. doi:https://doi.org/10.1021/acssuschemeng.8b02466. URL https://pubs.acs.org/doi/10.1021/acssuschemeng.8b02466.
[18] A. Rommerskirchen, Y. Gendel, M. Wessling, Single module flow-electrode capacitive deionization for continuous water desalination 60 34–37. doi:https://doi.org/10.1016/j.elecom.2015.07.018. URL https://linkinghub.elsevier.com/retrieve/pii/S1388248115001988.
[19] N. Köller, L. Mankertz, S. Finger, C. J. Linnartz, M. Wessling, Towards pilot scale flow-electrode capacitive deionization 572 117096. doi:https://doi.org/10.1016/j.desal.2023.117096. URL https://linkinghub.elsevier.com/retrieve/pii/S0011916423007282.
[20] C. Shi, H. Wang, A. Li, G. Zhu, X. Zhao, F. Wu, Process model for flow-electrode capacitive deionization for energy consumption estimation and system optimization 230 119517. doi:https://doi.org/10.1016/j.watres.2022.119517. URL https://linkinghub.elsevier.com/retrieve/pii/S0043135422014622.
[21] J. Ma, C. Zhai, F. Yu, Review of flow electrode capacitive deionization technology: Research progress and future challenges 564 116701. doi:https://doi.org/10.1016/j.desal.2023.116701. URL https://linkinghub.elsevier.com/retrieve/pii/S0011916423003338.
[22] N. Köller, M. Perrey, L. K. Brückner, P. Schäfer, S. Werner, C. J. Linnartz, M. Wessling, Comparison of current collector architectures for flow-electrode capacitive deionization 582 117595. doi:https://doi.org/10.1016/j.desal.2024.117595. URL https://linkinghub.elsevier.com/retrieve/pii/S0011916424003060.
[23] H. Strathmann, Ion-exchange membrane separation processes, membrane science and technology series, 1st edition, no. 9, Elsevier, ISBN 978-0-08-050940-2.
[24] H. Strathmann, A. Grabowski, G. Eigenberger, Ion-exchange membranes in the chemical process industry 52 (31) 10364–10379. doi:https://doi.org/10.1021/ie4002102. URL https://pubs.acs.org/doi/10.1021/ie4002102.
[25] B. Yuzer, H. Selcuk, G. Chehade, M. Demir, I. Dincer, Evaluation of hydrogen production via electrolysis with ion exchange membranes 190 116420. doi:https://doi.org/10.1016/j.energy.2019.116420. URL https://linkinghub.elsevier.com/retrieve/pii/S0360544219321152.
[26] S. Jiang, H. Sun, H. Wang, B. P. Ladewig, Z. Yao, A comprehensive review on the synthesis and applications of ion exchange membranes 282 130817. doi:https://doi.org/10.1016/j.chemosphere.2021.130817. URL https://linkinghub.elsevier.com/retrieve/pii/S0045653521012881.
[27] T. Luo, S. Abdu, M. Wessling, Selectivity of ion exchange membranes: A review 555 429–454. doi:https://doi.org/10.1016/j.memsci.2018.03.051. URL https://linkinghub.elsevier.com/retrieve/pii/S0376738817335779.
[28] T. Sata, Studies on ion exchange membranes with permselectivity for specific ions in electrodialysis 93 (2) 117–135. doi:https://doi.org/10.1016/0376-7388(94)80001-4. URL https://linkinghub.elsevier.com/retrieve/pii/0376738894800014.
[29] A. Rommerskirchen, B. Ohs, K. A. Hepp, R. Femmer, M. Wessling, Modeling continuous flow-electrode capacitive deionization processes with ion-exchange membranes 546 188–196. doi:https://doi.org/10.1016/j.memsci.2017.10.026. URL https://linkinghub.elsevier.com/retrieve/pii/S0376738817321774.
[30] A. Rommerskirchen, M. Alders, F. Wiesner, C. J. Linnartz, A. Kalde, M. Wessling, Process model for high salinity flow-electrode capacitive deionization processes with ion-exchange membranes 616 118614. doi:https://doi.org/10.1016/j.memsci.2020.118614. URL https://linkinghub.elsevier.com/retrieve/pii/S037673882031190X.
[31] A. Rommerskirchen, H. Roth, C. J. Linnartz, F. Egidi, C. Kneppeck, F. Roghmans, M. Wessling, Mitigating water crossover by crosslinked coating of cation-exchange membranes for brine concentration 6 (10) 2100202. doi:https://doi.org/10.1002/admt.202100202. URL https://onlinelibrary.wiley.com/doi/10.1002/admt.202100202.
[32] J. Ma, L. Chen, F. Yu, Environmental applications and perspectives of flow electrode capacitive deionization (FCDI) 335 126095. doi:https://doi.org/10.1016/j.seppur.2023.126095. URL https://linkinghub.elsevier.com/retrieve/pii/S1383586623030034.
[33] J. Zhang, L. Tang, W. Tang, Y. Zhong, K. Luo, M. Duan, W. Xing, J. Liang, Removal and recovery of phosphorus from low-strength wastewaters by flow-electrode capacitive deionization 237 116322. doi:https://doi.org/10.1016/j.seppur.20

19.116322. URL https://linkinghub.elsevier.com/retrieve/pii/S1383586619344120.

[34] T. M. Khoi, N. A. T. Tran, H. B. Jung, V. P. Huynh, Y. Kim, J. Hong, C.-Y. Yoo, H. S. Kang, Y. Cho, Selective and continuous ion recovery using flow electrode capacitive deionization with polymer multilayers functionalized ion exchange membrane 558 116626. doi:https://doi.org/10.1016/j.desal.2023.116626. URL https://linkinghub.elsevier.com/retrieve/pii/S0011916423002588.

[35] H. Zhang, Y. Li, J. Han, Y. Sun, M. He, Z. Hao, T. Jiang, B. Wang, W. Wang, M. Liu, Influence of ion exchange membrane arrangement on dual-channel flow electrode capacitive deionization: Theoretical analysis and experimentations 548 116288. doi:https://doi.org/10.1016/j.desal.2022.116288. URL https://linkinghub.elsevier.com/retrieve/pii/S0011916422007433.